THE JOURNAL OF BIOLOGICAL CHEMISTRY
Vol. 274, No. 46, Issue of November 12, pp. 32970–32974, 1999

Printed in U.S.A.

Manipulating the Amyloid-β Aggregation Pathway with Chemical Chaperones*

(Received for publication, July 21, 1999)

Dun-Sheng Yang‡, Christopher M. Yip§¶, T. H. Jackson Huang‖‡‡, Avijit Chakrabartty‖**, and Paul E. Fraser‡‖§§**

*From the ‡Centre for Research in Neurodegenerative Diseases, the §Department of Chemical Engineering and Applied Chemistry, the ¶Institute for Biometerials and Biomedical Engineering, the ‖Department of Medical Biophysics, and the **Ontario Cancer Institute, University of Toronto, Toronto, Ontario M5S 3H2, Canada*

Amyloid-β (Aβ) assembly into fibrillar structures is a defining characteristic of Alzheimer's disease that is initiated by a conformational transition from random coil to β-sheet and a nucleation-dependent aggregation process. We have investigated the role of organic osmolytes as chemical chaperones in the amyloid pathway using glycerol to mimic the effects of naturally occurring molecules. Osmolytes such as the naturally occurring trimethylamine *N*-oxide and glycerol correct folding defects by preferentially hydrating partially denatured proteins and entropically stabilize native conformations and polymeric states. Trimethylamine *N*-oxide and glycerol were found to rapidly accelerate the Aβ random coil-to-β-sheet conformational change necessary for fiber formation. This was accompanied by an immediate conversion of amorphous unstructured aggregates into uniform globular and possibly nucleating structures. Osmolyte-facilitated changes in Aβ hydration also affected the final stages of amyloid formation and mediated transition from the protofibrils to mature fibers that are observed *in vivo*. These findings suggest that hydration forces can be used to control fibril assembly and may have implications for the accumulation of Aβ within intracellular compartments such as the endoplasmic reticulum and *in vitro* modeling of the amyloid pathway.

Amyloid plaques are a central feature of Alzheimer's disease pathology and are considered to be a major factor in neuronal cell loss (1, 2). Ultrastructurally, plaques are fibrous masses composed primarily of the 40–42-residue amyloid-β (Aβ)[1] peptide. Aβ is derived by endoproteolysis of the integral membrane amyloid precursor protein that results in secretion of the peptide by normal cellular pathways as well as intracellular accumulation. Under pathogenic conditions, Aβ self-associates into a well defined supramolecular fibril with high β-sheet content (3). Aβ polymerization is considered to be a two-stage process initiated by the association of individual Aβ monomers into small nucleating "seeds" that is accompanied by a transition from a predominately random coil to an amyloidogenic β-sheet conformation (4, 5). Subsequent to nucleation, the Aβ seeds assemble in a chain-like manner to yield an intermediate protofibrillar structure (6–8), which may represent a common element of all amyloid fibrils (9, 10). Protofibril conversion into the ramified fibrils observed *in vivo* can be affected by factors such as the amyloid-binding apoE, which is an Alzheimer's disease risk factor (11); the relative quantity of the more amyloidogenic Aβ species (4); and other chaperone elements that may control Aβ self-association.

The observation that Aβ is generated within intracellular compartments, including the endoplasmic reticulum (12–15), which is the quality control site for protein folding, has prompted us to investigate the role of chemical chaperones in the Aβ folding pathway. Under stress conditions or exposure to denaturants, heat shock proteins and chemical chaperones assist in stabilizing correctly folded proteins. Through a process known as osmotic remediation (16), chemical chaperones or organic osmolytes, including carbohydrates, free amino acids, or methylamines (*e.g.* trimethylamine *N*-oxide (TMAO)), effectively control protein folding through a preferential hydration of exposed polypeptide backbone and side chains of partially unfolded structures (17). Chemical agents such as glycerol and polyethylene glycol mimic these hydration effects, which creates a thermodynamically unstable state due to the unfavorable entropic changes associated with the increased ordering of bound water molecules (18). This can be rectified by folding of the protein into its native conformation, which sequesters the exposed groups and excludes the osmolytes from the protein domain. As a result, the free energy of the native conformation is substantially lower than the unfolded state, which is demonstrated by the ability of glycerol to correct misfolded proteins within the endoplasmic reticulum (19). Hydration effects are equally important in protein polymerization where osmolytes are excluded through increased protein-protein interactions and can, for example, enhance the assembly and stability of microtubules (20). The preferential assembly of protein polymer subunits such as Aβ and tubulin is a product of their unique structure, which results in the fibrous aggregate being the lowest energy conformer. Our findings indicate that similar forces contribute to the initiation of the Aβ random coil-to-β-sheet transition and stabilization of the resulting aggregates. These observations suggest that chemical chaperones may be useful in modeling amyloid plaque formation and may have some bearing on the cellular events involved in fibril formation.

* This work was supported in part by grants from the Medical Research Council of Canada (to P. E. F., A. C., and C. M. Y.), the Ontario Mental Health Foundation and the Scottish Rite Charitable Foundation of Canada (to P. E. F.), Neurochem, Inc. (to P. E. F., and D.-S. Y.), and the Connaught Foundation (to C. M. Y.). The costs of publication of this article were defrayed in part by the payment of page charges. This article must therefore be hereby marked "*advertisement*" in accordance with 18 U.S.C. Section 1734 solely to indicate this fact.

‡‡ Supported by studentships from the National Sciences and Engineering Research Council and the Medical Research Council of Canada.

§§ To whom correspondence should be addressed: Centre for Research in Neurodegenerative Diseases, University of Toronto, 6 Queen's Park Crescent West, Toronto, Ontario M5S 3H2, Canada. Tel.: 416-978-0101; Fax: 416-978-1878; paul.fraser@utoronto.ca.

[1] The abbreviations used are: Aβ, amyloid-β; TMAO, trimethylamine *N*-oxide; NBD, *N′*-(7-nitrobenz-2-oxa-1,3-diazol-4-yl)ethylenediamine; TMAFM, tapping mode atomic force microscopy; AFM, atomic force microscopy.

EXPERIMENTAL PROCEDURES

Peptide Synthesis and Labeling—Amyloid-β peptide residues 1–40 (Aβ40) was synthesized and purified as described previously (21). Peptides were examined immediately following dissolution in aqueous buffer and following prolonged incubation at high concentration to promote small protofibrillar β-sheet aggregates. Aβ40 was labeled for fluorescence studies using *N*,*N*′-dimethyl-*N*-(iodoacetyl)-*N*′-(7-nitrobenz-2-oxa-1,3-diazol-4-yl)ethylenediamine (Molecular Probes, Inc.) as described (22). *N*′-(7-Nitrobenz-2-oxa-1,3-diazol-4-yl)ethylenediamine (NBD)-labeled peptide was purified by gel filtration chromatography and disaggregated in 10% hexafluoro-2-propanol, and stock solutions were stored at −20 °C.

Secondary Structure Analysis—The effects of TMAO (Sigma) and glycerol (BDH) on Aβ conformation were determined by CD. Peptides were dissolved to a final concentration of 50 μM in distilled water or 10 mM phosphate buffer (pH 7). Peptide solutions were combined with the TMAO at concentrations ranging from 50 to 150 μM and with glycerol ranging from 1.2 to 6 M (10–50% by volume). Spectra were collected following a 10-min equilibration period and after 48–72 h of incubation at room temperature. Spectra were acquired on a Jasco Model J-715 spectropolarimeter in a 0.1-cm path length cell over a wavelength range of 190–250 nm with a 1.0-nm bandwidth, 0.1-nm resolution, 1-s response time, and 20 nm/min scan rate. All spectra were corrected by subtraction of any contributions from buffer, glycerol, TMAO or polyethylene glycol.

Electron and Atomic Force Microscopy—Aβ aggregates were examined by phosphotungstic acid negative staining and platinum/carbon shadowing techniques as described previously (17). For shadowing studies, the samples were atomized onto freshly cleaved mica, immediately plunged into liquid nitrogen, and lyophilized to eliminate drying artifacts that could be caused by changes in peptide concentration. Dried preparations were platinum-coated in an Edwards E12E4 coater and viewed on a Hitachi H-7000 electron microscope operated with an accelerating voltage of 75 kV.

For tapping mode atomic force microscopy (TMAFM) studies, the peptides were dissolved in 25 mM phosphate buffer (pH 7) and then adjusted to the desired TMAO or glycerol content to a final peptide concentration of 2.5 μM. Approximately 10 μl of the peptide solution was transferred to a piece of freshly cleaved mica glued to a steel AFM sample mount. The sample was then immediately sealed in the TMAFM liquid cell, and the cell was filled with buffer solution. TMAFM imaging was conducted at room temperature using a combination contact/tapping mode liquid cell fitted to a Digital Instruments Nanoscope IIIA MultiMode scanning probe microscope. All images were acquired using 120-μm oxide-sharpened silicon nitride V-shaped cantilevers (type DNP-S, Digital Instruments Inc., Santa Barbara, CA) at a scan rate of ~2 Hz and a sampling rate of 256 or 512 points/scan line. Prior to use, the AFM tips were exposed to UV irradiation to remove adventitious organic contaminants from the tip surface. While *a priori* determination of the appropriate drive frequency is difficult owing to viscous coupling between the cantilever and the fluid medium, which gives rise to multiple broad resonance peaks, optimal imaging was achieved at a cantilever drive frequency of ~8.9 kHz.

Solubility Measurements—The aggregation state of Aβ under the various solvent conditions was examined by high speed centrifugation and assay of the soluble material using the fluorescent labeled peptide as indicator. Solutions containing 0.1 μM NBD-labeled Aβ40 and 10 μM unlabeled peptide were combined in 25 mM phosphate buffer (pH 7) containing from 0 to 6.0 M glycerol. NBD-labeled Aβ40 fluorescence spectra were acquired; the samples were centrifuged in a Beckman Airfuge at maximum velocity (135,000 × *g*) for 30 min; and the fluorescence spectra of the supernatants were measured. Spectra of control samples containing only Aβ40 were collected and subtracted from the NBD-labeled Aβ40 fluorescence to correct for the effects of light scattering. Steady-state fluorescence was measured at room temperature using a Photon Technology International QM-1 fluorescence spectrophotometer equipped with excitation intensity correction. Emission spectra from 500 to 600 nm were collected (λ_{ex} = 478 nm, 0.1 s/nm, 8-nm band pass for excitation and emission) using a 0.2 × 1-cm path length, 0.5-ml cuvette. To determine the effects of glycerol on the fluorescent probe, unconjugated NBD at 0.1 μM was measured under comparable conditions.

RESULTS AND DISCUSSION

Circular dichroism was used to evaluate the effects of the naturally occurring osmolyte TMAO and glycerol on Aβ conformation. When dissolved in aqueous buffers, Aβ40 initially exhibits a random coil conformation indicative of an unordered structure (Fig. 1*A*). Consistent with previous reports, the conformational changes of Aβ from random coil to β-sheet (21) and subsequent fibril formation (23) can take from hours to days depending on the particular peptide batch and incubation conditions. In contrast, adjusting the solution to 1.2 M glycerol (10%, v/v) resulted in an immediate folding of the peptide into the amyloid-associated β-conformer. Increasing the glycerol level to 3 or 6 M (25–50%, v/v) produced a linear increase in the β-sheet content as measured by the minima intensity at 218 nm (Fig. 1*A*). These effects were not due to increased peptide concentration caused by immiscibility in glycerol since CD studies conducted in which Aβ concentrations were doubled (from 50 to 100 μM) to replicate the 50% glycerol conditions revealed no change in the random coil structure of Aβ40 (data not shown). A similar change was observed for Aβ40 that had been preincubated to form β-sheet aggregates, which represent the early stages of fibril formation. In this case, elevating glycerol concentrations proportionally increased the preexisting β-sheet content, but to a slightly lesser quantitative degree as compared with the random coil-to-β-sheet conformational change (Fig. 1*B*). Identical results were obtained under all conditions in the presence of a low molecular mass (400 Da) polyethylene glycol at varying concentrations (data not shown). These results indicate that changes in protein hydration by chemical chaperones rapidly accelerate the conformational transition required for amyloid formation.

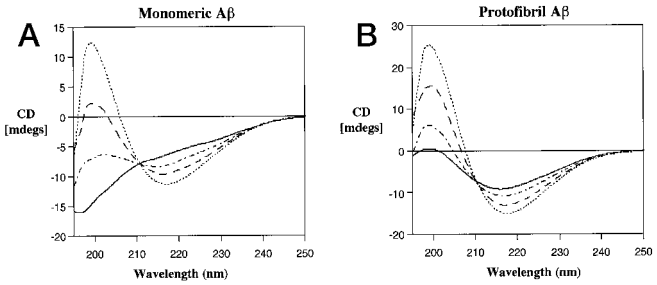

FIG. 1. *A*, CD of Aβ40 demonstrating the immediate conversion from random coil to a β-sheet conformation with increasing glycerol concentrations; *B*, conformational transitions of an incubated or "aged" Aβ40 comparable to the protofibril state indicating a similar effect of increasing the β-sheet content induced by glycerol-mediated solvation effects. Spectra are of the Aβ peptide in buffer (——) and in the presence of 1.2 M (– · –), 3.0 M (– – –), or 6.0 M (···) glycerol. *mdegs*, millidegrees.

Glycerol is a nonphysiological model of osmolyte activity, and we therefore investigated the effect of TMAO, which is found *in vivo* and acts to maintain correctly folded proteins in several species (17). TMAO produced a similar random coil-to-β-sheet transition as that seen with glycerol, but at significantly lower concentrations of 50–150 μM (corresponding to molar ratios of 1:1 and 1:3 peptide/TMAO) (Fig. 2*A*). Similar to glycerol, TMAO increased the quantity of the β-conformation with the preincubated peptide, which initially displayed a folded and aggregated structure (data not shown). The increases in β-sheet conformation by both TMAO and glycerol were found to be roughly linear as determined by the absorption at 218 nm (Fig. 2*B*). However, at the higher concentrations of TMAO, the proportion of the β-conformation appeared to be approaching a plateau. These findings suggest that TMAO is a more active compound in controlling the folding and aggregation state of Aβ, which may reflect a more potent effect of this osmolyte in an *in vivo* setting.

The morphological changes associated with the β-sheet conformation were assessed by TMAFM performed directly in aqueous buffer. TMAFM of Aβ in the absence of the chemical chaperones revealed irregular aggregate rafts with an approx-

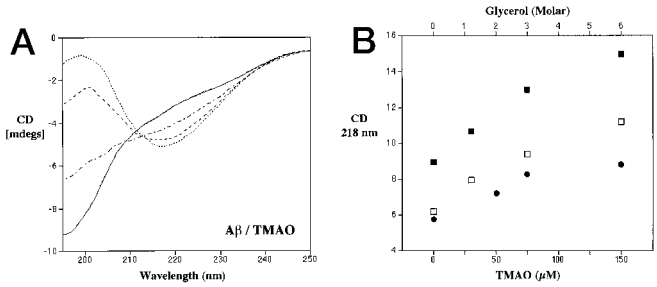

FIG. 2. *A*, CD of Aβ40 demonstrating the immediate conversion from random coil to a β-sheet conformation with increasing concentrations of TMAO. Control Aβ in buffer only (——) and Aβ/TMAO at molar ratios of 1:1 (– · –), 1:1.5 (– – –), and 1:3 (····) are indicated. *B*, proportional increases in the β-sheet conformation as measured by the absorption at 218 nm in the presence of TMAO (●) and glycerol (□) with Aβ initially in the random conformation and following preincubation prior to the addition of glycerol (■). *mdegs*, millidegrees.

imate thickness of 10 nm (Fig. 3*A*). The presence of aggregates was unexpected since it is generally assumed that the random coil conformation corresponds to a fully solvated and soluble Aβ monomer. Since the samples were not pretreated to remove small peptide aggregates (*e.g.* submicron filtration), these minor components could be present and serve as nuclei for nonspecific precipitation. Alternatively, the amorphous deposits may be due to adsorption of Aβ to the mica substrate used for TMAFM. The addition of either TMAO or glycerol at concentrations that produced the random coil-to-β-sheet transition, as confirmed by CD, resulted in a complete conversion of the amorphous Aβ aggregates to a mixture of protofibrils and small ellipsoidal particles (Fig. 3, *B* and *C*). The protofibrils varied in length and displayed a globular axial periodicity of ~100 Å that was comparable to their average diameter. These were morphologically similar to previously reported protofibrils (7, 8). However, judging from wider field scans, the ellipsoid aggregates predominated with dimensions of 50 × 60 × 15 Å (Fig. 3*C*, *arrow*). We noted that these dimensions are slightly overestimated due to convolution of the AFM tip shape with the aggregate shape.

Given an experimentally determined volume of ~45,500 Å^3, these ellipsoid particles represent Aβ tetramers or pentamers based on a calculated volume of ~10,000 Å^3 for an Aβ (residues 1–42) molecule folded into a two-stranded β-sheet. These may represent an aggregate of the Aβ dimer that has been shown to be stable under similar aqueous conditions (24). Comparable structures have been observed by AFM (25, 26) and have been termed Aβ-derived diffusible ligands, which may represent the most neurotoxic species (27). The position of these small aggregates on the amyloid pathway is presently unclear. A straightforward explanation would be that there is a linear relationship where these are the progenitors of the protofibrils that are generated by the direct polymerization of the ellipsoid aggregates. Alternatively, they may represent a side reaction with Aβ monomers shuttling between these and the protofibrils.

Assembly of the nucleating aggregates to form protofibrils is considered to be the slow kinetic phase of the amyloid pathway (28). This is followed by the thermodynamic phase with the transition to compacted amyloid fibrils, a process that may also be affected by osmolyte-induced hydration. Previous AFM and negative stain electron microscopy studies have defined protofibrils as truncated and highly flexible fibrillar structures that are the precursors to plaque-related fibrils (6, 7, 8). Following preincubation of a concentrated Aβ40 solution, we have observed similar aggregates of similar morphology using platinum/carbon shadowing techniques (Fig. 4*A*). Such protofibrils ranged in length from 1 to 100 nm and were poorly contrasted, suggesting that they have a low profile. The addition of glycerol resulted in a rapid conversion to straight compacted fibrils that extended over several hundred nanometers (Fig. 4*B*) and occasionally displayed helical twisting (*arrowheads*). Exposure to chemical chaperones such as glycerol also significantly improved the image contrast of the fibrils, presumably as a result of their compaction into more defined tubular assemblies. Although some curved protofibril-like structures remained following glycerol treatment, there was a complete conversion to the longer fibrils following several hours of incubation (data not shown). Elongation occurred at a significantly greater pace as compared with the several days required to convert Aβ protofibrils in the absence of the glycerol chaperone.

To obtain a quantitative measure of aggregation under our experimental conditions, centrifugation was employed using Aβ labeled with the fluorescent probe NBD. Our previous fluorescence resonance energy transfer studies have indicated that the low concentrations of the fluorophore-labeled Aβ do not interfere with the kinetics of fibril formation or the morphology of the resulting aggregates (22). In the current study, similar peptide solutions containing excess unlabeled (10 μM) and NBD-labeled (0.1 μM) Aβ were used. Prior to centrifugation, the fluorescence intensity increased linearly with increasing concentrations of glycerol, with the fluorescence at 6 M glycerol being approximately twice that of the buffer-only sample (Fig. 5). This increase was due to glycerol-induced changes in the quantum yield of NBD as shown by the response of the unconjugated label under these conditions. Following centrifugation, a 97% decrease in fluorescence was observed, indicating that the peptides are almost completely aggregated. This was the case for the glycerol-containing samples as well as the initial aqueous solution, which is consistent with the amorphous aggregates observed by AFM. This is likely due to the fact that the samples were not pretreated, for example, by filtration to remove nonspecific aggregates, which would have allowed examination of the more direct conversion of soluble monomer to Aβ aggregate. However, the results presented here with untreated samples suggest that the conversion to the β-sheet particles, which are induced by solvation changes, may involve a shuttling of monomers from the unordered structure to the nucleating aggregates. An analogous situation may occur with the diffuse-to-senile plaque Aβ interconversion that is seen *in vivo*, and the use of chemical chaperones may be useful in modeling this aspect of the amyloid pathway.

Cumulatively, these results demonstrate that changes in the solvation state of the Aβ peptide affect several aspects of the amyloidogenic pathway. In general terms, amyloid fibrils are initiated by the destabilization of a normal cellular protein that leads to a partially unfolded intermediate. This can be accelerated by point mutations, as has been shown for lysozyme (29) and transthyretin (30), which are deposited as systemic plaques. If uncorrected, the unfolded intermediate will ultimately assemble into the β-sheet aggregates that initiate fibril formation. It has been proposed that chemical chaperones may, in part, regulate amyloid formation by stabilizing the lower energy native conformer to reduce the levels of unfolded proteins that are required for the amyloidogenic pathway. This is consistent with the observation that naturally occurring organic osmolytes inhibit the conversion of the cellular prion protein (PrP^C) to the protease-resistant and amyloid-forming PrP^{SC} associated with transmissible encephalopathies (31, 32). Similar stabilization by glycerol of misfolded mutant transmembrane proteins within the endoplasmic reticulum has been demonstrated for the chloride transporter associated with cystic fibrosis (33, 34) and aquaporins related to nephrogenic diabetes (35).

Although stabilizing native conformations of larger proteins

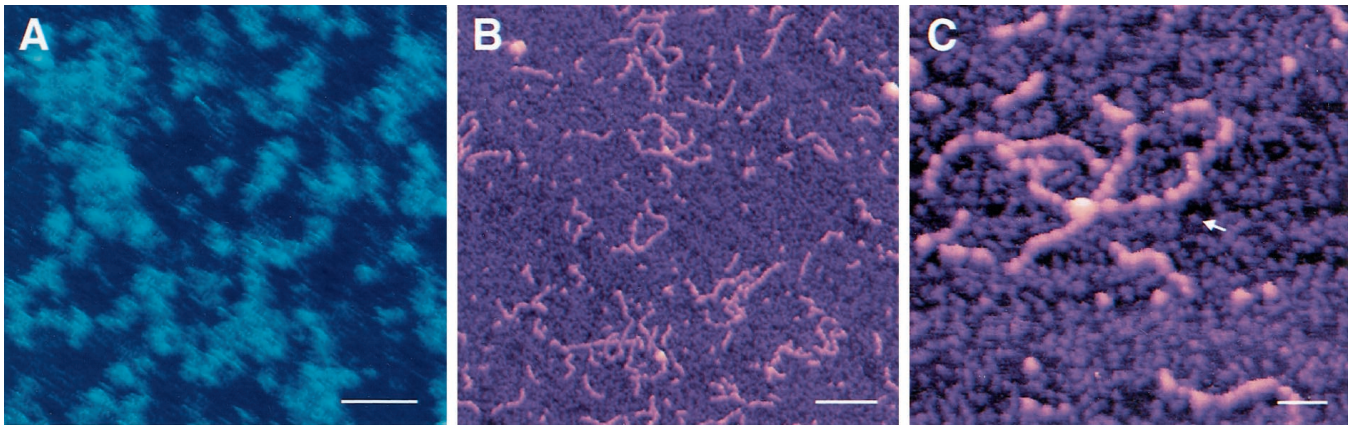

FIG. 3. **Morphological changes in peptide aggregates induced by chemical chaperones.** *A*, atomic force microscopy of Aβ40 (2.5 μM) in phosphate buffer demonstrating the amorphous aggregates. *B*, a wide field scan of an identical Aβ40 peptide in 6.0 M glycerol revealing the formation of protofibrils and smaller nonfibrillar aggregates. Identical structures were observed in the presence of 150 μM TMAO. *C*, enlarged view of the protofibrils indicating the globular morphology and the discrete ellipsoidal aggregates (*arrow*) representing the tetrameric/pentameric aggregate. *Scale bars* are 100 nm in *A*, 2500 nm in *B*, and 500 Å in *C*.

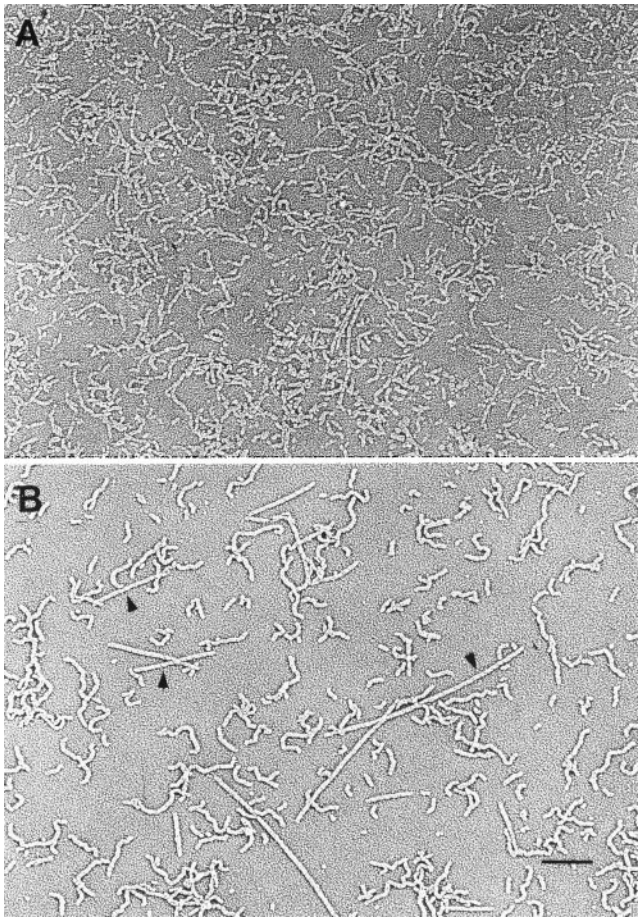

FIG. 4. *A*, rotary platinum/carbon shadowing electron microscopy of Aβ40 demonstrating the presence of protofibrils in a preincubated or aged preparation; *B*, transition to amyloid fibrils in 6.0 M glycerol showing the formation of elongated and rigid fibers that occasionally exhibited a helical twisting (*arrowheads*). *Scale bar* is 1000 Å.

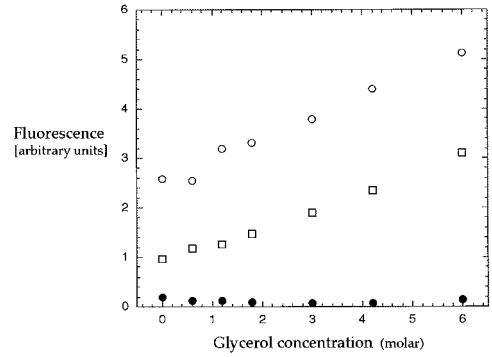

FIG. 5. **Insolubility of the unstructured and fibrillar aggregates monitored by a fluorescent labeled Aβ peptide tracer.** Peptides incubated in aqueous phosphate buffer or with increasing concentrations of glycerol were subjected to high speed centrifugation. Precipitation of peptide was observed in all cases as shown by the loss of fluorescence observed in the initial solutions (○) as compared with the supernatant fluorescence following centrifugation (●). The increase in fluorescence at higher glycerol concentrations is due to changes in the probe as shown by similar changes in unconjugated label (□).

can affect amyloid formation, it is likely that Aβ does not have a conventional conformation and may therefore exist in an unfolded and possibly amorphous state. Therefore, if unchecked by cellular control elements, the peptide will gradually deposit as diffuse and eventually senile plaques. Our results indicate that solvation changes induced by chemical chaperones such as the naturally occurring TMAO and the *in vitro* model provided by glycerol rapidly accelerate the major steps in the amyloidogenic pathway. These include both the early nucleation and conformational events as well as the protofibril-to-fiber conversion. This may be unique to proteins that normally exist in polymeric forms as shown by chemical chaperone-mediated assembly of tubulin into microtubules and their subsequent resistance to urea denaturation (20). The significance of our findings is that they reveal additional contributors to Aβ fibril formation and therefore provide an additional tool to manipulate this pathway. Such information could potentially be used to develop or accelerate cellular models of Aβ aggregation and the assessment of agents that modulate fibril formation.

REFERENCES

1. Selkoe, D. J. (1997) *Science* **275,** 630–631
2. Kisilevsky, R., and Fraser, P. E. (1997) *Crit. Rev. Biochem. Mol. Biol.* **32,** 361–404
3. Inouye, H., Fraser, P. E., and Kirschner, D. A. (1993) *Biophys. J.* **64,** 502–519
4. Jarrett, J. T., Berger, E. P., and Lansbury, P. T., Jr. (1993) *Biochemistry* **32,** 4693–4697
5. Lomakin, A., Teplow, D. B., Kirschner, D. A., and Benedek, G. B. (1997) *Proc. Natl. Acad. Sci. U. S. A.* **94,** 7942–7947
6. Stine, W. B., Jr., Snyder, S. W., Ladror, U. S., Wade, W. S., Miller, M. F., Perun, T. J., Holzman, T. F., and Krafft, G. A. (1996) *J. Protein Chem.* **15,** 193–203
7. Harper, J. D., Wong, S. S., Lieber, C. M., and Lansbury, P. T. (1997) *Chem. Biol.* **4,** 119–125
8. Walsh, D. M., Lomakin, A., Benedek, G. B., Condron, M. M., and Teplow, D. B. (1997) *J. Biol. Chem.* **272,** 22364–22372
9. Sunde, M., Serpell, L. C., Bartlam, M., Fraser, P. E., Pepys, M. B., and Blake,

C. C. F. (1997) *J. Mol. Biol.* **273,** 729–739
10. Blake, C. C. F., and Serpell, L. (1996) *Structure* **4,** 989–998
11. Schmechel, D. E., Saunders, A. M., Strittmatter, W. J., Crain, B. J., Hulette, C. M., Joo, S. H., Pericak-Vance, M. A., Goldgaber, D., and Roses, A. D. (1993) *Proc. Natl. Acad. Sci. U. S. A.* **90,** 9649–9653
12. Cook, D. G., Forman, M. S., Sung, J. C., Leight, S., Kolson, D. L., Iwatsubo, T., Lee, V. M., and Doms, R. W. (1997) *Nat. Med.* **3,** 1021–1023
13. Hartmann, T., Bieger, S. C., Bruhl, B., Tienari, P. J., Ida, N., Allsop, D., Roberts, G. W., Masters, C. L., Dotti, C. G., Unsicker, K., and Beyreuther, K. (1997) *Nat. Med.* **3,** 1016–1020
14. Wild-Bode, C., Yamazaki, T., Capell, A., Leimer, U., Steiner, H., Ihara, Y., and Haass, C. (1997) *J. Biol. Chem.* **272,** 16085–16088
15. Skovronsky, D. M., Doms, R. W., and Lee, V. M. (1998) *J. Cell Biol.* **141,** 1031–1039
16. Burg, M. B. (1995) *Am. J. Physiol.* **268,** 983–996
17. Wang, A., and Bolen, D. W. (1997) *Biochemistry* **36,** 9101–9108
18. Timasheff, S. N. (1993) *Annu. Rev. Biophys. Biomol. Struct.* **22,** 67–97
19. Brown, C. R., Hong-Brown, L. Q., and Welch, W. J. (1997) *J. Clin. Invest.* **99,** 1432–1444
20. Sackett, D. L. (1997) *Am. J. Physiol.* **273,** R669–R676
21. McLaurin, J., Franklin, T., Chakrabartty, A., and Fraser, P. E. (1998) *J. Mol. Biol.* **278,** 183–194
22. Huang, T. H. J., Fraser, P. E., and Chakarbartty, A. (1997) *J. Mol. Biol.* **269,** 214–224
23. Harper, J. D., Lieber, C. M., and Lansbury, P. T., Jr. (1997) *Chem. Biol.* **4,** 951–959
24. Garzon-Rodriguez, W., Sepulveda-Becerra, M., Milton, S., and Glabe, C. G. (1997) *J. Biol. Chem.* **272,** 21037–21044
25. Roher, A. E., Chaney, M. O., Kuo, Y. M., Webster, S. D., Stine, W. B., Haverkamp, L. J., Woods, A. S., Cotter, R. J., Tuohy, J. M., Krafft, G. A., Bonnell, B. S., and Emmerling, M. R. (1996) *J. Biol. Chem.* **271,** 20631–20635
26. Kowalewski, T., and Holzman, D. M. (1999) *Proc. Natl. Acad. Sci. U. S. A.* **96,** 3688–3693
27. Lambert, M. P., Barlow, A. K., Chromy, B. A., Edwards, C., Freed, R., Liosatos, M., Morgan, T. E., Rozovsky, I., Trommer, B., Viola, K. L., Wals, P., Zhang, C., Finch, C. E., Krafft, G. A., and Klein, W. L. (1998) *Proc. Natl. Acad. Sci. U. S. A.* **95,** 6448–6453
28. Evans, K. C., Berger, E. P., Cho, C. G., Weisgraber, K. H., and Lansbury, P. T., Jr. (1995) *Proc. Natl. Acad. Sci. U. S. A.* **92,** 763–767
29. Booth, D. R., Sunde, M., Bellotti, V., Robinson, C. V., Hutchinson, W. L., Fraser, P. E., Hawkins, P. N., Dobson, C. M., Radford, S. E., Blake, C. C. F., and Pepys, M. B. (1997) *Nature* **385,** 787–793
30. Lai, Z., Colon, W., and Kelly, J. W. (1996) *Biochemistry* **35,** 6470–6482
31. DebBurman, S. K., Raymond, G. J., Caughey, B., and Lindquist, S. (1997) *Proc. Natl. Acad. Sci. U. S. A.* **94,** 13938–13943
32. Tatzelt, J., Prusiner, S. B., and Welch, W. J. (1996) *EMBO J.* **15,** 6363–6373
33. Brown, C. R., Hong-Brown, L. Q., Biwersi, J., Verkman, A. S., and Welch, W. J. (1996) *Cell Stress Chaperones* **1,** 117–125
34. Sato, S., Ward, C. L., Krouse, M. E., Wine, J. J., and Kopito, R. R. (1996) *J. Biol. Chem.* **271,** 635–638
35. Tamarappoo, B. K., and Verkman, A. S. (1998) *J. Clin. Invest.* **101,** 2257–2267